

Study of Castor oil-based Auxetic Polyurethane Foams for Cushioning Applications

V Chaithanya Vinay^{1,2}, Mohan Varma D S^{1,2*}, Mohammed Rehaan Chandan^{3*}, Ponsubha Sivabalan², Amit Kumar Jaiswal², Sai Swetha³, Alina Sionkowska⁴ and Beata Kaczmarek⁴

¹*School of Mechanical engineering (SMEC), VIT Vellore, India*

²*Centre for Biomaterials Cellular & Molecular Theranostics (CBCMT), VIT Vellore, India*

³*Colloids and Polymer Research Group, School of Chemical Engineering (SCHEME), VIT Vellore, India*

⁴*Department of Biomaterials and Cosmetic Chemistry, Faculty of Chemistry, Nicolaus Copernicus University in Torun, Torun, Poland*

Correspondence: Dr. D S Mohan Varma
School of Mechanical Engineering, CBCMT,
VIT Vellore, Tamil Nadu.

Email: mohandamu@gmail.com

Tel: +91-9789846850

Correspondence: Dr. Mohammed Rehaan Chandan
Colloids and Polymer Research Group, School of Chemical Engineering (SCHEME),
VIT Vellore, India,
Email: md.rehaanchandan@vit.ac.in

Abstract:

This work involves the study of mechanical and antibacterial properties of auxetic polyurethane (APU) foams synthesized using castor oil (CO) to ascertain its suitability as a seat cushion in wheelchairs. Firstly, CO-based PU foams (PU-CO) were synthesized by substituting 25% synthetic polyol with CO in a polyol blend. Conventional PU foams and PU-CO foams were then converted to auxetic foams using triaxial compression and heating. The properties such as chemical composition, microstructure, thermal, mechanical and antibacterial properties of the foams were analyzed. It was seen that addition of CO increased the antibacterial and mechanical properties of the foam. Castor oil-based auxetic (CO-APU) foams showed highest compression strength and storage modulus. An increase in thermal stability of the PU-CO is also observed as compared to PU foams. These CO-APU foams could be a better alternative to conventional PU foams for wheelchair seat cushions and in hospital bed applications.

This article has been accepted for publication and undergone full peer review but has not been through the copyediting, typesetting, pagination and proofreading process which may lead to differences between this version and the [Version of Record](#). Please cite this article as doi: [10.1002/pi.6259](https://doi.org/10.1002/pi.6259)

Keywords: auxetic foams, castor oil, antibacterial, thermo-mechanical property, seat cushions

1. INTRODUCTION

PU foams are commonly used for rehabilitation applications such as wheelchair seat cushions, hospital beds, prosthetic liners in stump socket interface etc., for cushioning and comfort. Wheelchair users sit for long periods and therefore pressure relief is most important requirement in a cushion. One of the major problems faced by users of wheelchairs and prosthetic limbs are pressure ulcers. Pressure ulcers are injuries to the skin due to pressure along with shear and friction stresses. If pressure ulcers are left untreated, it can be life-threatening. Soft tissue protection over the skin area is necessary particularly for individuals who are bedridden and/or chair bound ^[1].

Various materials are being used to improve the comfort for wheelchair users. However, problems such as thinning of foams and excessive sweating still persist. Thinning of foams leads to improper distribution of stresses, and excessive sweating causes infections at the interface between the skin and the foams. Novel materials such as auxetic foams are being explored for use in rehabilitation applications ^[2]. Auxetic foams are known to enable uniform pressure distribution, high indentation resistance and high shear stiffness compared to conventional foams ^[3]. Lowe and Lakes ^[3] found that lower volumetric compression ratio of 2.2 showed the ideal pressure distribution. However, the type of raw or input foam and its density influenced the properties of the auxetic foams. Auxetic foams also exhibited higher fracture toughness, synclastic behavior and higher acoustic absorption and can be used in various applications ^[4]. Lakes fabricated the first metallic and polymeric auxetic foams. Several researchers followed his work and explored various methods to fabricate auxetic foams ^[5-6]. Auxeticity can be achieved through triaxial compression followed by heat treatment or through geometric honeycomb patterns, rotating rigid and chiral structures, etc. Works by various researchers have shown that auxetic materials can be made to have varying mechanical properties by varying the process parameters^[7-12]. This implies that these materials can be customized for a given application.

Properties of PU foams are affected mainly due to raw materials used to synthesize the foam such as fillers, stabilizers, chain extenders and cross-linking agents. Adverse environmental impacts are caused by the extensive use of polymers derived from petroleum. Therefore, there is a huge interest in the development of new environment-friendly polymers with low cost and controlled life span. Conventional PU foams are made of polyols and diisocyanate. These foams can be converted to biodegradable PU foams using vegetable oils like castor oil, palm oil and, soy^[13-14]. Researchers have also explored other additives like bark and corn starch^[15], and biopolyols like cellulose/starch^[16] and sunflower^[17] (*Helianthus annuus* L). Water-blown porous biodegradable PU foams can also be made with palm oil-based polyol^[18]. Green synthesis from Kraft lignin^[19] and modified tung oil, were also used in flexible PU foams synthesis^[20]. Al-

Mamun et al.,^[21] found castor oil plant or seed (*ricinus communis*) could minimize the growth of bacterial infections. Researchers have found that PU-CO foams are biodegradable and also exhibit antibacterial property^[21]. Therefore, in this work, CO is used in the synthesis of PU foams as it can result in foams that are biodegradable and antibacterial. Moreover, CO is easily available and is affordable.

Several researchers have explored methods to fabricate APU foams. The fabrication process of metallic and polymeric auxetic foams was first described by Lakes^[5,22]. Chan & Evans^[6] explored auxetic foam fabrication techniques and introduced a multi stage fabrication method which reduces surface creasing while fabricating large auxetic foams. Scarpa et al.^[23] used piston-cylinder for axial compression of the samples during the conversion process. They used compression ratios up to around 90% followed by heating up to the softening temperatures. Duncan et al.^[12] showed that use of through-thickness pins in fabrication provides greater in-plane compression control. Li & Zeng^[24] used styrene-acrylo-nitrile (SAN) particles in auxetic conversion and showed that the addition of SAN particles ensured faster conversion of the PU foam to APU foam. There are other methods like chemo-mechanical process^[25] and steam based methods for closed cell foams^[26] for the conversion of PU foams to APUs. In this work, multi stage fabrication method is used to fabricate APUs.

Image processing techniques (Digital Image Correlation) by video capturing are commonly used for the measurement of Poisson's ratio values of PU and APU foams. Most researchers have used image processing and correlation methods to calculate the Poisson's ratio values of the foams^[10,24,27]. In this work, videos of foam samples were captured and the images were used to determine Poisson's ratio. Mechanical characterization of APU foams has been performed by many researchers^[12,23,28,29]. Duncan et al.,^[12] and Scarpa et al.,^[23] reported higher compression strength of auxetic foams when compared to conventional foams in quasi-static compression and impact tests. Bezazi & Scarpa^[28,29] found that in high cycle fatigue loading, auxetic foams had less loss in rigidity than conventional polymeric foams. Martz et al.,^[30] found that the auxetic foams have higher damping capacity than conventional foams. It was seen^[31] that APU foams fabricated using lower compression factors had less loss of thickness under low cycle fatigue loading when compared to APU foams fabricated using higher compression ratios. Therefore, in this work, compression ratios not exceeding three were used to fabricate APU foams.

Antibacterial studies on PU foams have been performed by some researchers. Generally PU foams with chitosan, triclosan, CO and silver chloride etc., exhibit antibacterial properties^[21,32,33]. *Ricinus communis*, commonly known as castor oil plant belongs to spurge family (Euphorbiaceae) and is common throughout tropical and warm temperature regions of the world. This plant has antibacterial property which makes it an attractive candidate to cure

various diseases. The roots, leaves and seed oil of *Ricinus communis* have potential medicinal benefits and can be used for inflammation treatment, hypoglycemic, appendicitis, epilepsy, hemorrhoids, diarrhea, intestinal obstructions and liver disorders^[34-36]. Zarai et al., have studied the antibacterial effect of CO against twelve microbial species and they showed that CO inhibits bacterial growth. Their study also analyzed the strong antibacterial effect against three species - *Bacillus subtilis*, *Staphylococcus aureus* and *Enterobacter cloacae*^[37]. Momoh et al., found that the inherent functional groups and active chemical compositions such as tannin, phenol, saponin, cyanogenic glycoside and flavonoids couple enhances the antibacterial property of CO^[38]. The aim of this work is to explore the possibility of using CO in the synthesis of auxetic PU foams to take advantage of the biodegradability and antibacterial properties of CO. While auxetic properties can be tuned to ensure required pressure distribution in seat cushions, presence of CO can possibly inhibit the growth of infections which is a major concern in persons who are wheelchair bound for long periods.

In this work, flexible PU foams with CO additives were synthesized. These foams were then converted to auxetic PU foams using methodology described by Chan & Evans^[6]. FTIR, Morphological analyses (SEM), Dynamic Mechanical Analysis (DMA), uniaxial compression tests and antibacterial studies were performed on the CO-APU foams and compared to conventional foams. Poisson's ratios of all the foams were determined using image analysis^[24] and compared to conventional PU foams.

2. EXPERIMENTAL SECTION

2.1 Synthesis of foams:

Flexible PU foams are generally made from polyol, diisocyanate and catalyst blends. In this work, PU foams and PU-CO foams were made using methodology described in Sharma et al.^[39]. PU foams were synthesized from polyol and diisocyanate whereas PU-CO foams were synthesized from polyol blend containing 25 wt% CO and 75 wt% synthetic polyol and diisocyanate^[39]. Industrial grade castor oil was procured from the Falcon essential oils, Bangalore, India.

2.2 Thermal analysis

TG-DTG (Thermo gravimetric-derivative thermo gravimetric) analysis was performed using *Seiko thermo-analyser (model SII 7200)* to find the softening temperature of the foams. PU and PU-CO foam samples of nearly 2.2 milligrams weight were heated up to 600°C temperature at a 10°C/min heating rate in a high pure nitrogen atmosphere. Softening temperatures for both the samples were determined and used in the auxetic conversion process. Both the PU and PU-CO foams showed thermal stability until 200°C in TG-DTG analysis. Therefore, a temperature 200°C was selected for the fabrication process.

2.3 Fabrication of auxetic PU foams

Synthesized PU foams were converted to APU foams using thermo-mechanical process which involved triaxial compression and multi-stage heating. In the first stage of compression, the foams of $140 \times 95 \times 30 \text{ mm}^3$ volume were squeezed inside an aluminum box of volume $120 \times 80 \times 20 \text{ mm}^3$ and then closed with aluminum plate to maintain a volumetric compression ratio or compression factor (CF) of 2.07. Foams of $155 \times 105 \times 35 \text{ mm}^3$ volume were squeezed inside the same aluminum box and closed with an aluminum plate for a compression ratio of 2.96. An industrial furnace is initially pre-heated up to 200°C temperature. The aluminum box containing the compressed foam is then inserted into the furnace for 30 min. The foam is then cooled to room temperature followed by stretching for about 10 minutes. The heating and stretching process is then repeated once more. This fabrication process is adopted from Smith et al.,^[40] by varying process parameters. Using the above process, conventional PU foams and PU-CO foams are converted to auxetic foams.

2.4 Measurement of Poisson's ratio

Poisson's ratio of the foams were measured by capturing the video of the samples where one end of the foam was stretched up to nearly 30 mm while the other end was fixed to a wooden board. Thereafter, the video was converted to a series of images. Finally, using a MATLAB code, the boundary of the foam at different stages of stretching was found (Fig. 1). The displacement at the horizontal and vertical mid-lines were then measured and used to compute the Poisson's ratio.

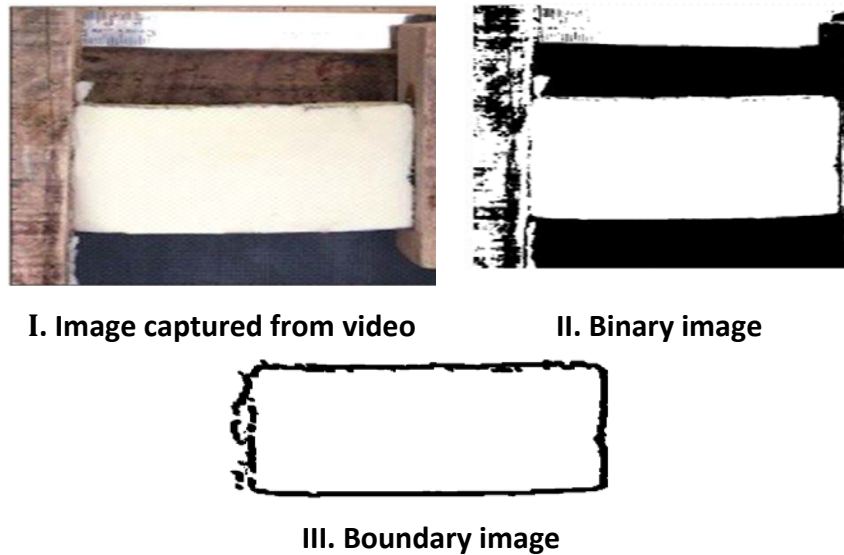


Fig. 1: Figures showing (I) image captured from video and (II) processed using image processing techniques (MATLAB) to determine the boundary (III) of the foam sample.

2.5 Fourier Transform Infrared (FTIR) analysis

FTIR spectral analysis was performed to investigate the chemical structure and different functional groups. FTIR spectra were recorded for PU foams and auxetic foams using FTIR (*Shimadzu Crop I Raffinity¹*) spectrophotometer from 400-4000 cm^{-1} wavenumbers at 30 scans per specimen with 4 cm^{-1} resolution. FTIR samples of foams were prepared by pressing the foam samples with Potassium Bromide (KBr) to form pellets.

2.6 Scanning Electron Microscopy (SEM)

Cellular morphologies of PU, auxetic PU foam (APU), PU-CO and auxetic PU-CO (CO-APU) samples were found using Scanning Electron Microscope (SEM) of *Carl Zeiss, Germany*. Samples were made into rectangular specimens and sputter-coated with gold particles (thin layer) on a specimen surface before observation.

2.7 Uniaxial compression tests:

Uniaxial compression tests were performed using mechanical testing machine of *Z.05 model, Zwick/Roell, Germany*. Stress-strain curves were captured at loading under room temperature for the samples of PU, PU-CO, APU and CO-APU foams (auxetic foams with two different compression ratios). Foams were placed between the two discs of machine and compressed with the strain rate of 1 mm min^{-1} at initial force of 0.01 N. These tests were conducted for all the foams up to 80% strains. A standard sample size of 50 mm x 50 mm x 20 mm was used.

2.8 Dynamic Mechanical Analysis (DMA)

DMA was carried out in a *Seiko instruments-Sii Nano Technology*. Foam samples of dimensions 10 x 8 x 2.5 mm^3 were tested using an initial frequency of 1 Hz and a compression clamp. The samples were heated at a rate of 5 $^{\circ}$ C per min from 30 to 120 $^{\circ}$ C.

2.9 Antibacterial susceptibility tests

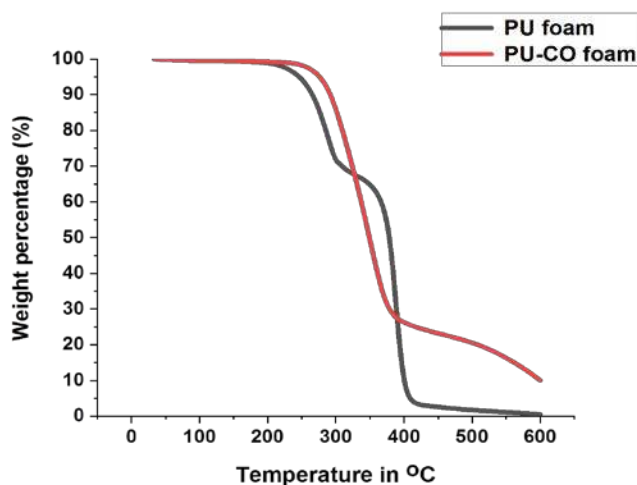
The antibacterial activity of all foam samples against both gram positive of *Staphylococcus aureus* and *Staphylococcus epidermidis* and gram negative of *Pseudomonas aeruginosa* and *Escherichia coli* bacterial strains were studied and compared *in vitro* using microbroth dilution method. The bacterial strains were inoculated into 10 ml of nutrient broth (*Hi-Media Laboratories, India*) and incubated in an orbital shaking incubator (*CIS-24 PLUS LCD - incubator*) for 24 h at 37 $^{\circ}$ C. The freshly prepared overnight bacterial cultures were diluted in 0.9% sterile saline solution and bacterial suspensions were adjusted to 1.5×10^6 CFU/ml using ELISA plate analyzer (Readwell TOUCH, ROBONIK) at $\lambda=600$ nm. After dilution, the samples (PU, PU-CO and CO-APU) were immersed into different wells of sterile 48-well plates containing the bacterial suspensions (1.5×10^6 CFU/ml) and incubated at 37 $^{\circ}$ C for 24 h under constant agitation. In

control wells, only bacterial suspensions were taken. After incubation of 24 h, the samples were removed from the wells and 20 μ l of each bacterial suspension were inoculated onto nutrient agar plate (Hi-Media Laboratories, Mumbai-India) and incubated for about 24 hrs at 37 $^{\circ}$ C. At the end of incubation period the bacterial colonies were enumerated by eye and the total amount (CFU/ml) of colonies were observed for each sample.

3. RESULTS AND DISCUSSION

3.1 Thermo gravimetric-Derivative thermo gravimetric (TG-DTG) analysis:

TG-DTG plots (Fig.2) show the variation in the percent weight of the sample with increase in temperature. The rapid decrease in the weight of the foams indicates the softening temperature. PU foams showed a multi-stage softening (at 280 $^{\circ}$ C and 390 $^{\circ}$ C) and PU-CO showed softening at 360 $^{\circ}$ C. In the case of PU foams, the first peak at 280 $^{\circ}$ C indicates the decomposition of urea and urethane bonds while the second peak at around 390 $^{\circ}$ C represents the polyether group breakdown [41]. Presence of CO in the PU sample alters the polymer morphology as CO has shorter chain length as compared to synthetic polyol. Introduction of shorter molecules in PU leads to an increase in 1st decomposition temperature. Similar results were observed by Shaik et. al [42] for PU-CO foam which shows 1st degradation at around 360 $^{\circ}$ C and onset of 2nd degradation around 480 $^{\circ}$ C. The results indicate that the inclusion of CO increases the thermal stability of the foam i.e., the CO based PU foam start to decompose at a slightly higher temperature than the conventional PU foam.



(a)

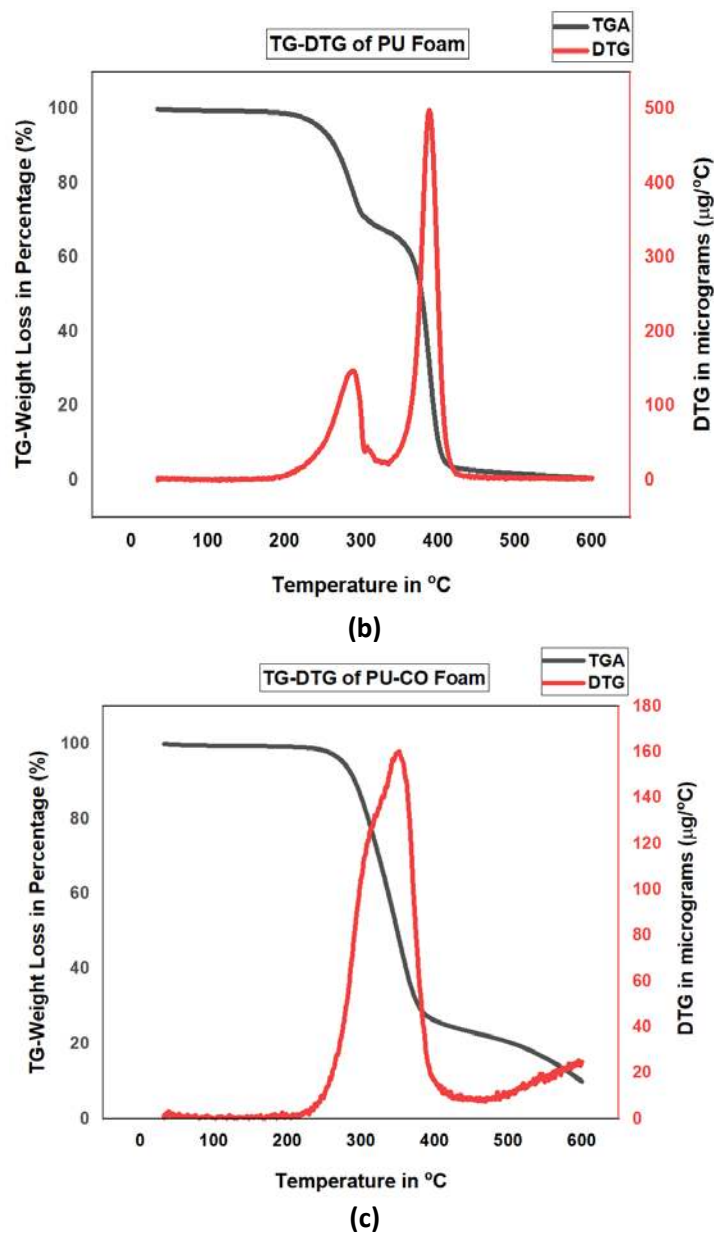


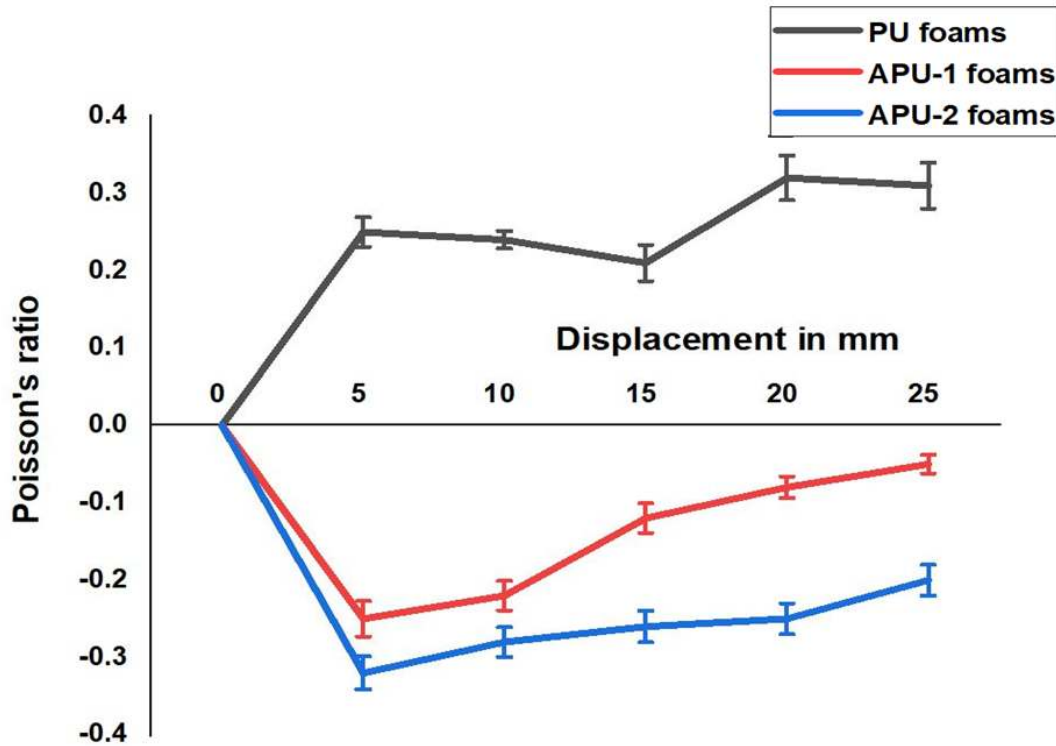
Fig. 2: TGA-DTG analysis of PU and PU-CO foams: Temperature versus weight percentage of PU and PU-CO foams (a) obtained from thermo gravimetric analyzer and thermographs of PU (b) and PU-CO (c) foams.

3.2 Poisson's ratio:

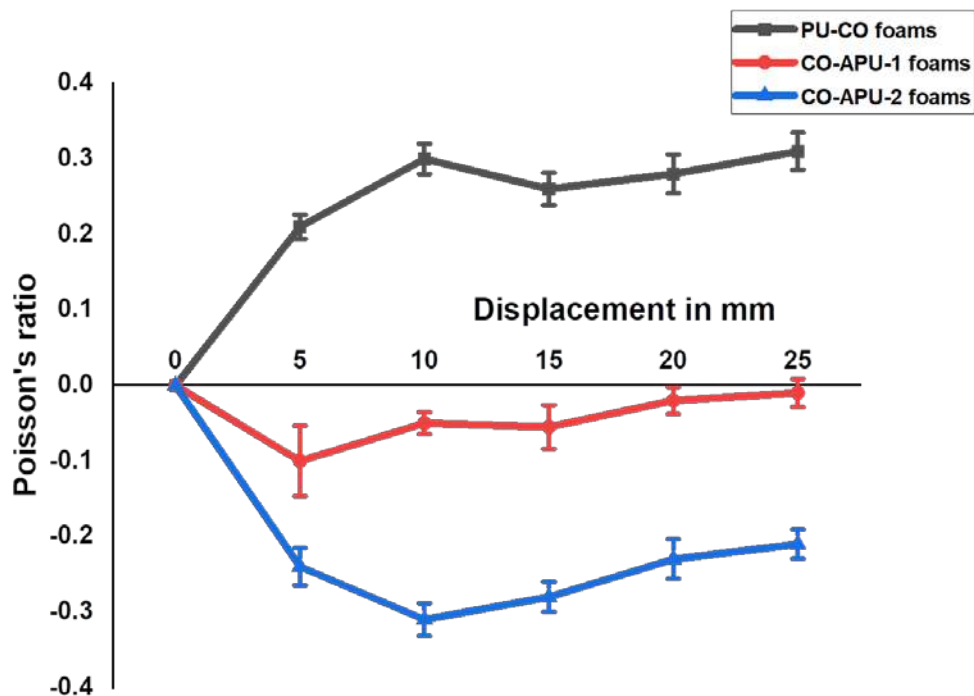
Poisson's ratio results of PU, PU-CO, APU and CO-APU foams are shown in Figs 3(a) and 3(b). Auxetic foams were made using two different compression factors: 2.07 (CO-APU-1) and 2.96 (CO-APU-2). In both APU and CO-APU, foams fabricated using higher compression ratio showed relatively higher auxetic effect. When PU foams are subjected to triaxial compression, the pores of the foams are filled with the buckled ribs. The foam then undergoes a permanent set while heating. In case of higher compression factors, the number of ribs that buckle and fill the voids

are higher. When tension is applied in the longitudinal direction, the unbuckling of the ribs causes expansion in the lateral direction. This effect is more in case of higher CF auxetic foams due to the presence of higher number of ribs in the same volume of the foam.

It can be seen that, in all the auxetic foams, the auxetic effect reduced with increase in displacement. Initially, expansion of all the buckled ribs contributes to the auxetic effect. Once a buckled rib is completely unbuckled, it does not contribute to the auxetic effect. As the displacement increases, more ribs are completely unbuckled and the auxetic effect is reduced.



(a)

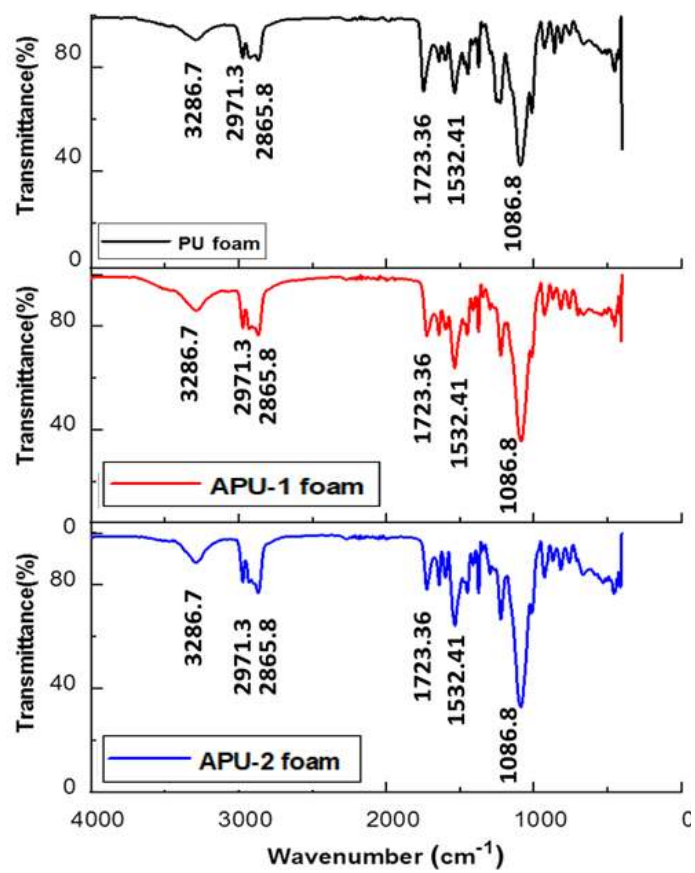


(b)

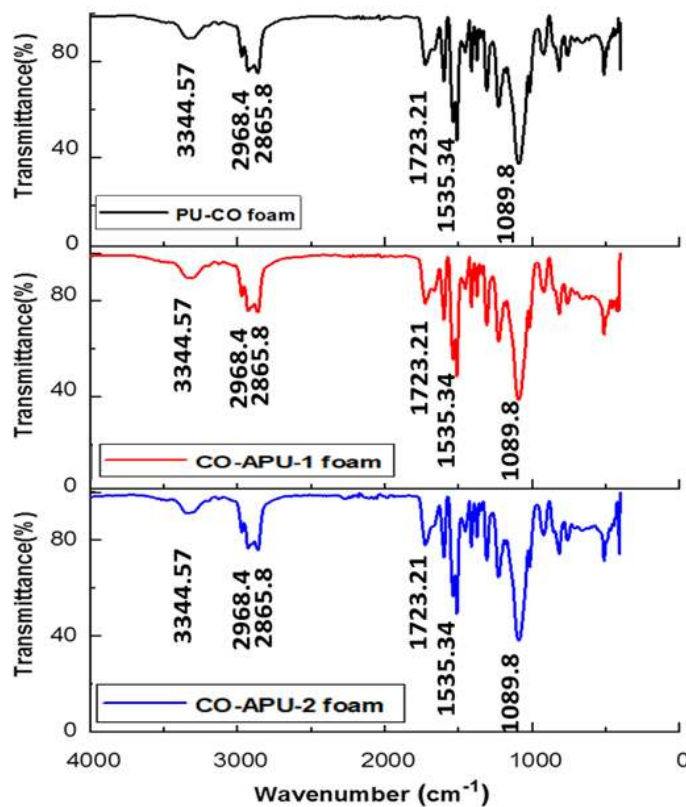
Fig.3: Poisson's ratio vs displacement curves for (a) PU and APU, and (b) PU-CO and CO-APU foams.

3.3 Fourier Transform Infrared (FTIR) analysis

FTIR results show that there is no significant change in the chemical structure of the foams before and after conversion to auxetic foams. As expected, the results showed (Fig. 4) difference in PU and PU-CO foams although the difference is not prominent. In the case of PU and APU foams, the peak at 3286.7 cm^{-1} refers to N-H stretch and peaks at 2971.3 and 2865.8 cm^{-1} originates from C-H stretch, peak at 1723.36 cm^{-1} refers to C=O groups and the peak at 1532.41 cm^{-1} corresponds to N-H stretching. The peak at wave number 1086.85 cm^{-1} is a result of C-O-C stretching. For CO-PU foams, peak at 3344.57 cm^{-1} refers to O-H stretching and the peaks at 2968.45 and 2860.63 cm^{-1} refers to C-H stretch and peak at 1723.21 cm^{-1} represents C=O group, peak at 1535.34 cm^{-1} represents N-H bending and the peak at 1089.78 cm^{-1} indicates C-O-C stretching.



(a)



(b)

Fig.4: FTIR spectra for (a) PU and APU foams, (b) PU-CO and CO-APU foams

3.4 Scanning Electron Microscopy (SEM)

Cellular morphology of all foams was studied using SEM (Fig.5). Auxetic foams had buckled ribs (Fig.5. b, c, e and f) due to the triaxial mechanical compression and heating process. Buckling is high for auxetic foams with higher compression factor (CF) 2.96 (Figs c and f) and the pores were filled with buckled ribs. This phenomenon is same for both PU and PU-CO foams when these are converted to auxetic foams (APU and CO-APU).

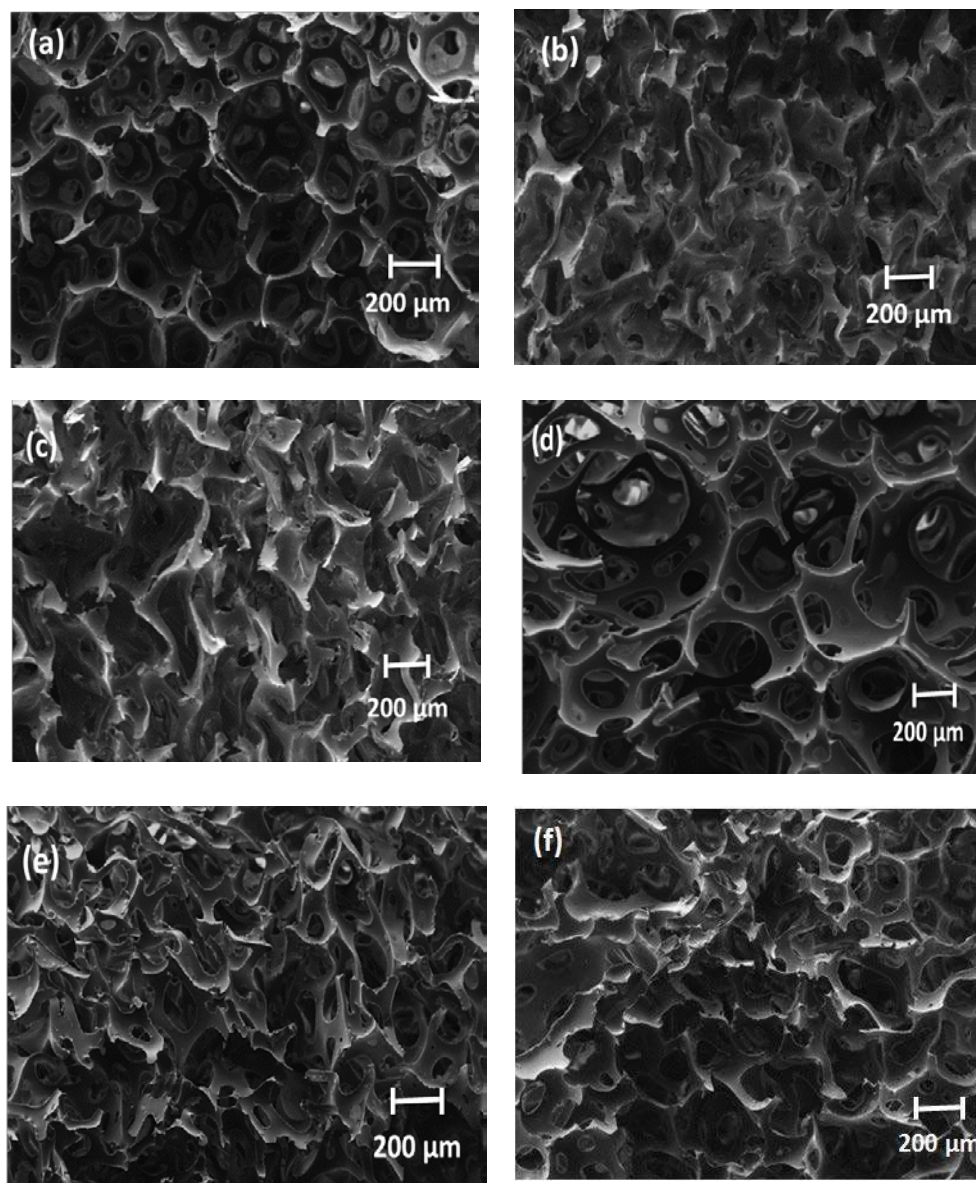
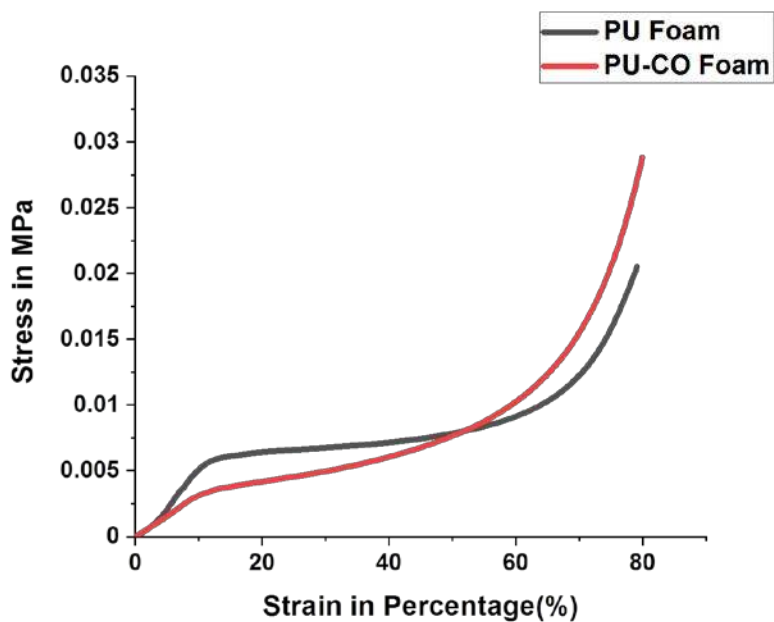


Fig.5: SEM images (100 X) for conventional PU foams and auxetic PU foam, (a) PU foam, (b) APU-1 foam, (c) APU-2 foam, (d) PU-CO foam, (e) CO-APU-1 foam, (f) CO-APU-2 foam

3.5 Uniaxial compression tests:

The compression test data shows that the response of PU and PU-CO foams to compression (Fig.6(a)) is similar to that of most other conventionally available PU foams with a relatively linear stress-strain relationship in the first stage (elastic region) followed by a plateau region (elastic collapse) and densification (strain hardening). With the addition of CO, the PU-CO foam had reduced plateau than that of PU foam. The reduction in plateau region in the case of PU-CO can be attributed to the chemical reactions during fabrication of PU-CO^[39].

After conversion to auxetic foams, the response to compression shows that there is almost no plateau region or elastic collapse in both PU and PU-CO foams (Fig. 6(b) & 6(c)). Initially auxetic foams exhibit large deformations (up to approx. 25% of strain) and after certain strain limit (from 25 to 30% of strains), they exhibit higher stiffness. Auxetic foams are soft at lower strains and are becoming stiffer as the strain increased. This change in the mechanical behavior of the foam is due to the buckling of the ribs during the fabrication process. When the foam is triaxially compressed, the ribs buckle and occupy the voids in the foam. The heating and cooling process causes these structures to set in that fashion (as is shown in the SEM images, Fig 5). During the compression tests, the buckled ribs in the APU foams ensure deformation for a longer period than conventional foams thereby avoiding the elastic collapse (plateau region) in the stress-strain curve. These additional deformations due to the buckled ribs occur until approximately 30% strain (Fig. 6(b)). Beyond this strain, the voids are completely filled and hence more force is required for further deformation. Similar response to compression was seen in both APU and CO-APU foams (Figs. 6(d) and 6(e)).



(a)

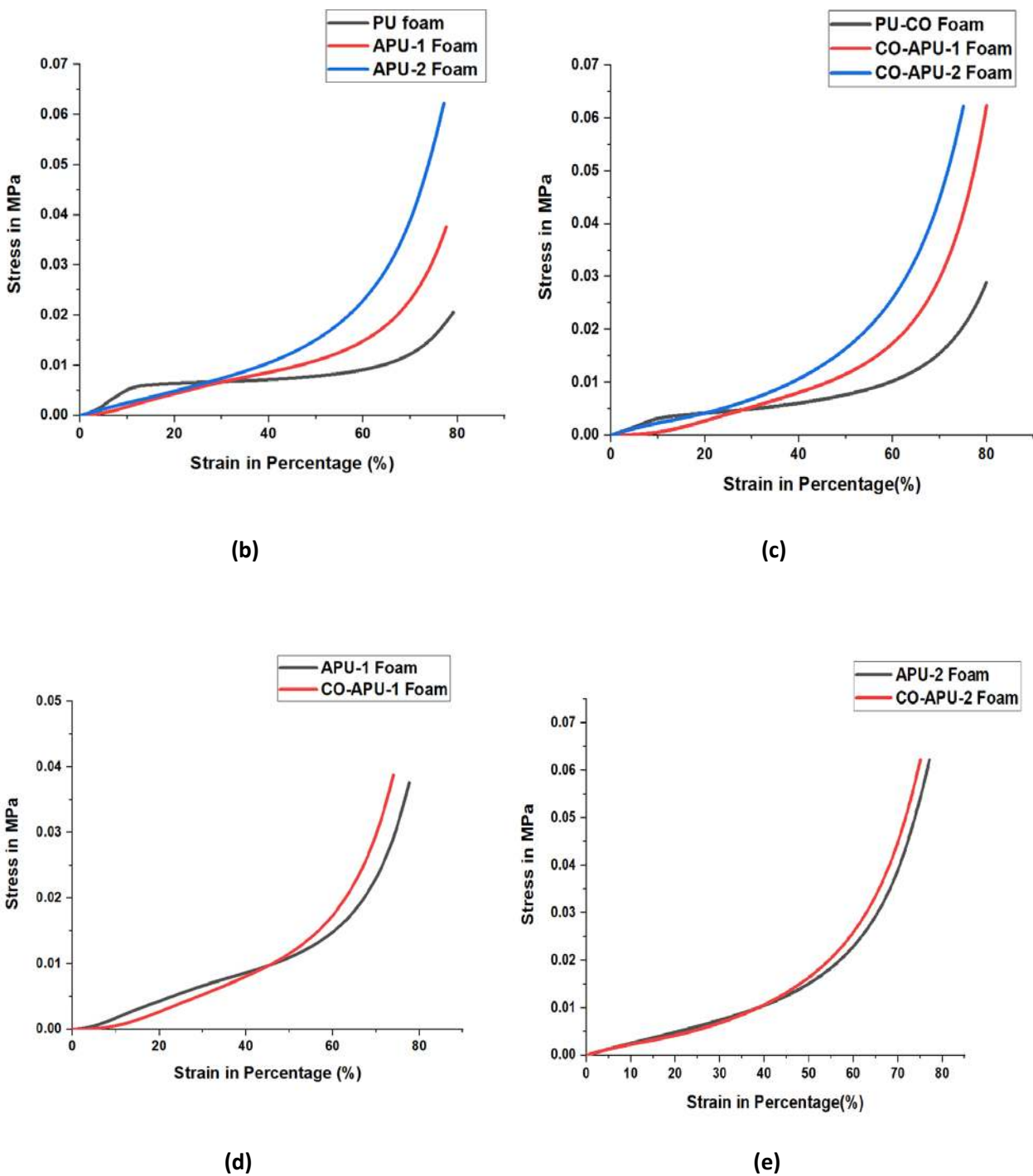


Fig.6: Stress-strain curves for (a) PU and PU-CO foams, (b) PU and APU (2.07 and 2.96 CF) foams, (c) PU-CO and CO-APU (2.07 and 2.96 CF) foams (d) APU and CO-APU (2.07 CF) and (e) APU and CO-APU(2.96 CF) foams.

3.6 Dynamic Mechanical Analysis (DMA)

The ratio between loss and storage modulus, $\tan \delta$, of a viscoelastic material describes its damping^[43-44]. Fig.7 shows the $\tan \delta$ versus temperature of all the foam samples determined using DMA. As expected, both PU and PU-CO foams showed gradual decrease in damping with increase in temperature. It can be seen that addition of CO had improved the damping characteristics of the PU foam. Sharma et al.^[39] also showed that the presence of CO increases the viscous dissipation than the recovery (elastic) of the CO based foams. Upon conversion of the foams to auxetic foams, APU and CO-APU foams showed reduction in damping when compared to PU and PU-CO foams respectively. This reduction of damping can be attributed to more number of cross linkages in the micro structure of APU and CO-APU foams which makes it more dense / elastic. Between the two CO-APU foams, the foam with higher compression ratio (2.96 CF CO-APU) showed higher damping properties possibly due to higher content of CO in a given volume of foam. APU foams showed almost similar damping after 50°C temperature.

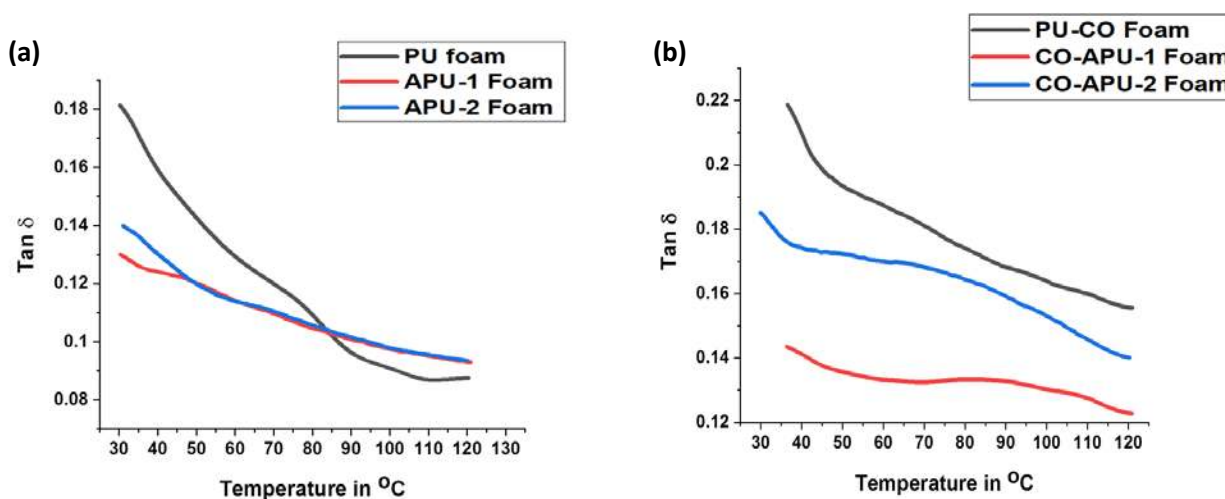


Fig. 7: $\tan \delta$ versus temperature of (a) PU and APU foams (b) PU-CO and CO-APU foams

3.7 Antibacterial properties:

The PU and APU foams mostly showed heavy or partially heavy growth of bacteria indicating insufficient antibacterial activity (Fig 8. and Tables 1-4). APU foams with 2.96 CF showed better antibacterial activity in comparison to the ones with CF of 2.07. CO-based foams showed a much better antibacterial effect when compared to PU foams. CO-APU foams with higher CF showed greater antibacterial effect than the other CO-based foams. In general, bacterial growth decreased with the increase of the CF. The increase in density (due to higher CF) of the foam increases the content of CO in the same volume of the foams. The compact sample network possibly had become a barrier for bacteria spreading throughout the foams and enables the biofilm formation. Overall, PU-CO and CO-APU foams displayed sufficient antibacterial effect against gram positive strains over gram negative strains.

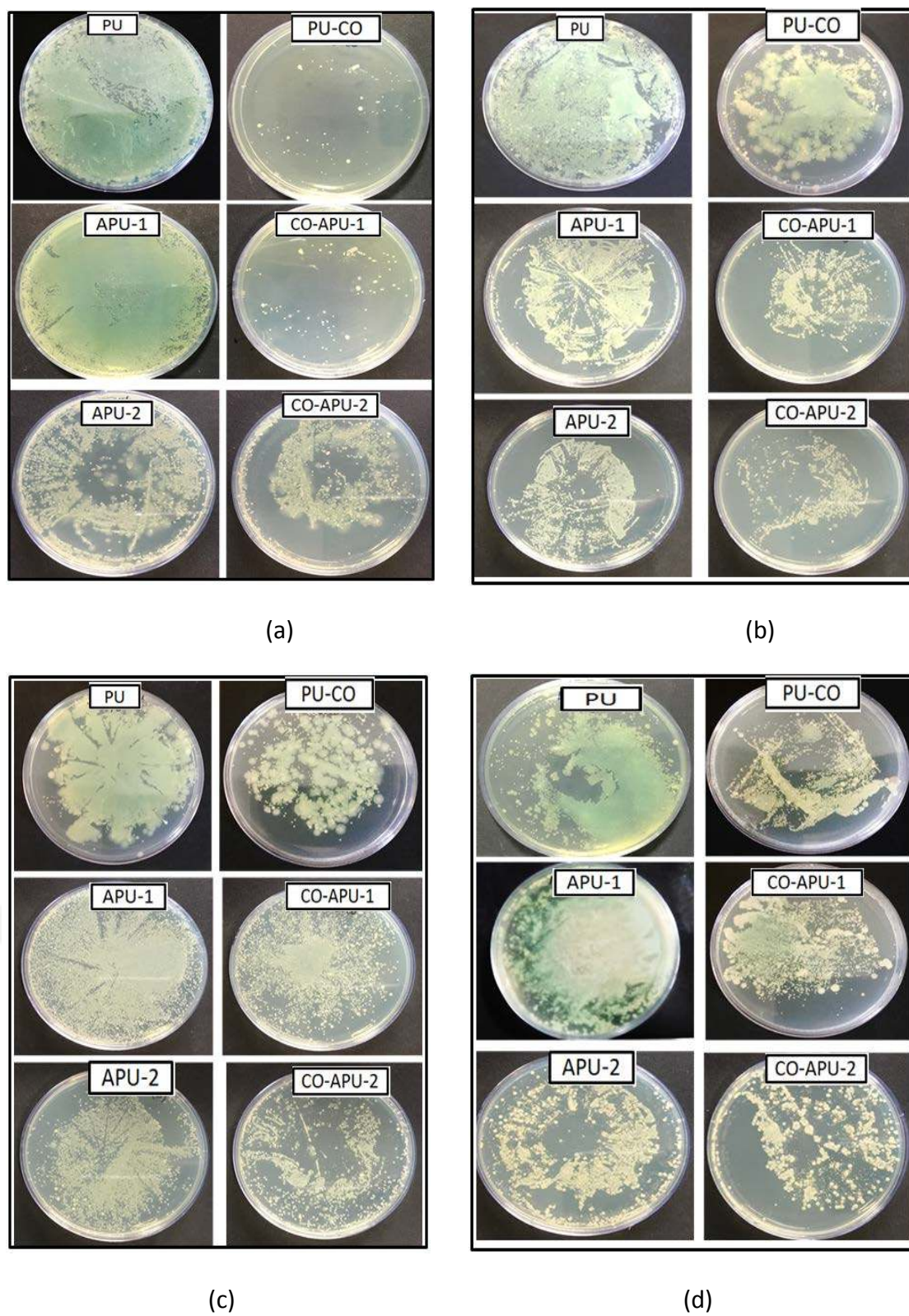


Fig.8: Antibacterial assessment of PU, PU-CO, APU-1, CO-APU-1, APU-2 and CO-APU-2 against (a) *S. Aureus*, (b) *E. Coli*, (c) *S. Epidermidis* and (d) *P. Aeruginosa* bacteria.

	Sample name	Growth	Assessment
S. aureus	PU	Heavy	Insufficient effect
	APU-1	Heavy	Insufficient effect
	APU-2	Partially heavy	Partially insufficient effect
	PU-CO	Partially medium	Limit of efficacy
	CO-APU-1	Partially medium	Limit of efficacy
	CO-APU-2	Partially medium	Partially limit of efficacy

Table 1: Antibacterial assessment against *S. aureus*.

	Sample name	Growth	Assessment
E.coli	PU	Heavy	Insufficient effect
	APU-1	Partially heavy	Partially Insufficient effect
	APU-2	Partially heavy	Partially insufficient effect
	PU-CO	Heavy	Insufficient
	CO-APU-1	Partially heavy	Partially limit of efficacy
	CO-APU-2	Partially heavy	Partially limit of efficacy

Table 2: Antibacterial assessment against *E.coli*.

	Sample name	Growth	Assessment
S. Epidermidis	PU	Heavy	Insufficient effect
	APU-1	Heavy	Insufficient effect
	APU-2	Partially heavy	Partially insufficient effect
	PU-CO	Partially medium	Partially limit of efficacy
	CO-APU-1	Partially medium	Partially limit of efficacy
	CO-APU-2	Medium	Limit of efficacy

Table 3: Antibacterial assessment against *S. Epidermidis*.

	Sample name	Growth	Assessment
P.Aeruginosa	PU	Heavy	Insufficient effect
	APU-1	Heavy	Insufficient effect
	APU-2	Partially heavy	Partially insufficient effect
	PU-CO	Partially medium	Partially limit of efficacy
	CO-APU-1	Partially medium	Partially limit of efficacy
	CO-APU-2	Partially medium	Partially limit of efficacy

Table 4: Antibacterial assessment against *P.aeruginosa*.

4. CONCLUSION

Our study indicates that the use of CO in the fabrication of auxetic foams results in higher strength (CO-APU-2 has higher compressive strength (0.06 MPa; Fig 6(c) when compared to PU foam (0.02 MPa; Fig 6(b)) and better antibacterial properties (Fig 8 and Tables 1-4) than in conventional PU foam. Moreover, the use of CO makes the foam biodegradable. In the present work, samples of size 120 mm x 80 mm x 20 mm were made and tested. Further studies on large (seat size) foams and testing using standardized methodologies for seat cushions^[45] and human trials to study pressure distribution capacity of large foams are needed. Overall, our results are encouraging and indicate a possibility of realizing a low-cost, easy to manufacture smart seat cushions that are antibacterial and provide better stress distribution and comfort to the users.

ACKNOWLEDGEMENTS

The authors would like to thank Council of Scientific & Industrial Research, Government of India, for assistance provided in the form of CSIR Direct- SRF. File Number: 09/844(0064)/2019-EMR-I

REFERENCES

- [1] T.W.Hsu, S.Y.Yang, J.T.Liu, C.T.Pan, Y.S. Yang, *Assi. Tech.*, **2016**. 1-8.
- [2] B.Wang, C.Zhang, C.Zeng, L. D.Kramer, A. Gillis, (Florida state university). *Patent No. US 9.486,333 B2*. **2016**.
- [3] A. Lowe, R. S. Lakes, *Cell. Polym.*, **2000**, 157-167.
- [4] Z.Wang, C.Luan, G.Liao, J.Liu, X.Yao, J. Fu, *Adv.Eng. Mater.*, **2020**. 1-23.
- [5] R. Lakes, *Reports*, **1987**,1038-1040.
- [6] N.Chan, K. E.Evans, *J. Mat. Sci.*, **1997**, 5945–5953.
- [7] N.Chan, K. E.Evans, *J. Cellular Plast.*, **1998**, 231-260.
- [8] N.Chan, K. E.Evans, *J. Cellular Plast.*, **1999**, 131-165.
- [9] I.Chekkal, M.Bianchi, C.Remillat, F. Bécot, L.Jaouen, F. Scarpa, *. Acta Acust.uni. with Acust.*, **2010**. 266- 274.
- [10] H. C.Cheng, F.Scarpa, T. H.Panzera, I.Farrow, H.X.Peng, *Basic solid state phy.*, **2018**.
- [11] J. Choi, R. Lakes, *Inter. J. of Frac.*, **1996**, 73-83.

- [12] O.Duncan, L.Foster, T.Senior, T.Allen, A. Alderson, *Pro. Eng.*, **2016**, 384 – 389.
- [13] M.Spontón, N.Casis, P.Mazo, B.Raud, A.Simonetta, L.Ríos, *Inter. Biodeteri. & Biodegra.*, **2013**, 85-94.
- [14] V.Sharma, P. Kundu, *Prog. in Poly.Sci.*, **2008**,1199–1215.
- [15] J.Ge, W.Zhong, Z.Guo, W. Li, K.Sakai, *J. of Appl.Poly.Sci.*, **1999**,2575-2580.
- [16] J.David, L.Vojtova, K. Bednarik, J. Kucerik, M.Vavrova, J.Janca,. *Environ. Chem. Letters*, **2010**, 381-385.
- [17] B. Das, U.Konwar, M.Mandal, N. Karak, *Indus. Crops and Prod.*, **2013**, 396– 404.
- [18] W.Seng Ng, C. S.Lee, C. H.Chuah, S. F. Cheng, *Indus. Crops and Prod.*, **2017**, 65–78.
- [19] P.Cinelli, I. Anguillesi, A.Lazzeri, *Euro.Poly. Jour.* , **2013**,1-10.
- [20] V. R. Silva, M. A. Mosiewicki, M. I. Yoshida, M. C. Silva, P. M. Stefani, N. E.Marcovich, *Poly. Test.*, **2013**, 665–672.
- [21] M. A. Al-Mamun, Z. Akter, M. J. Uddin, K. M. Ferdaus, K. M. Hoque, Z. Ferdousi, *BMC Comple. & Alter. Med.*, **2016**, 1-10.
- [22] E. A. Friis, R. S. Lakes, J. B. Park, *J. Mater. Sci.*, **1988**,4406-4414.
- [23] F. Scarpa, P. Pastorino, A. Garelli, S. Patsias, Ruzzene., *Basic solid state phy.*, **2005**, 681–694.
- [24] Y. Li, C. Zeng, *Polymer*, **2016**, 98-107.
- [25] J. N. Grima, D. Attard, R. Gatt, R. N. Cassar,. *Adv.Eng.Mat.*, **2009**, 533-535.
- [26] D. Fan, M. Li, J. Qiu, H. Xing, Z. Jiang, T. Tang, *Appl. Mat. and Inter.*, **2018**, 1-10.
- [27] J. Lisiecki, T. Błazejewicz, S. Kłysz, G. Gmurczyk, P. Reymer, G. Mikułowski, *Basic Solid State Phy*, **2013**, 1988–1995.
- [28] A. Bezazi, F. Scarpa, *Inter.J. Fatigue*, **2007**, 922–930.
- [29] A. Bezazi, F. Scarpa, *Inter.J. Fatigue*, **2009**, 488–494.
- [30] E. O. Martz, R. S. Lakes, J. B. Park, *Cell. Polym.*,**1996**, 349-364.
- [31] V. C. Vinay, D. S. Varma, *J. Ind.Institute of Sci.*, **2019**, 511-518.

- [32] S. K. Bhullar, M. Orhan, M. B. Jun, *Nanotechnology-Driven Engineered Materials: New Insights*, Apple Academic Press: Waretown, **2019**, Chapter 9, 1-14.
- [33] V. S. Dagostin, D. L. Golçalves, C. B. Pacheco, W. B. Almeida, I. P. Thomé, C. T. Pich, *Mat. Sci. Eng.C*, **2010**, 705-708.
- [34] M.L. Dhar, M.N. Dhar, B.L. Dhawan, B. Mehrotra, C. Ray, *Ind. J. of Exp. Biology*, **1968**, 232-247.
- [35] F. Capasso, N. Mascolo, A. A. Izzo, T. S., *British J. of Pharma.*, **1994**, 1127-1130.
- [36] S. Rampadarath, D. Puchooa, *Asian Pacific J. of Trop. Biomed.*, **2016**, 100-107.
- [37] Z. Zarai, I. B. Chobba, R. B. Mansour, , A. Békir, N. Gharsallah, A. Kadri, *Lipids in Heal. and Dis.*, **2012**, 1-7.
- [38] A. O. Momoh, M. K. Oladunmoye, T. T. Adebolu, *Bulletin of Environ., Pharma.and Life Sci. ,* **2012**, 21-27.
- [39] C. Sharma, S. Kumar, U. A. Raman, V. K. Aswal, S. K. Rath, G. Harikrishnan, *J. of Appl. Polym.Sci.*, **2014**, 1-8.
- [40] C. W. Smith, J. N. Grima, K. E. Evans, *Acta Mater.* **2000**, 4349–4356.
- [41] C. Sharma, S. S. Edatholath, A. R. Unni, T. U. Patro, V. K. Aswal, S. K. Rath, *J. of Appl. Polym. Sci.*, **2016**, 1-9.
- [42] A. H. Shaik, R. Jain, S. Manchikanti, K. Krishnamoorthy, D. K. Bal, A.Rahaman, S. Agashe, M. R. Chandan, *Chemistry Select*, **2020**, 3959-3964
- [43] A. Leszczynska, K. Pielichowski, *J. of Ther.Anal. and Calorim.*, **2008**, 677–687.
- [44] K. N. Raftopoulos, J. Pagacz, Jan Ozimek, S. Koutsoumpis, S. Michałowski, E. Hebda, J. Pielichowski, K. Pielichowski, *Polym.Bulletin*, **2019**, 2887–2898.
- [45] S. J. Hillman, J. Hollington, N. Crossan, C. T. Sánchez, *Assi. Tech.* **2017**, 1-7.